The Winter Annual Meeting of the ASME
Sixth Annual Symposium on Haptic Interfaces for Virtual Environment and Teleoperator Systems
Dallas, Texas, November 15-21, 1997.

# MECHANISM DESIGN FOR GLOBAL ISOTROPY WITH APPLICATIONS TO HAPTIC INTERFACES

**Leo J. Stocco, Septimiu E. Salcudean and Farrokh Sassani***

Department of Electrical and Computer Engineering,
*Department of Mechanical Engineering,
The University of British Columbia, Vancouver, British Columbia, Canada V6T 1Z4
leos@ee.ubc.ca, tims@ee.ubc.ca, sassani@mech.ubc.ca

## ABSTRACT

A new global isotropy index (*GII*) is proposed to quantify the configuration independent isotropy of a robot's Jacobian or mass matrix. The matrix is scaled to homogenize the physical units, to tailor it to the demands of the application and to choose optimum actuator parameters. A new discrete global optimization algorithm is also proposed to optimize the *GII* without placing any conditions on the objective function. The algorithm is used to establish design guidelines and a globally optimum architecture for a planar haptic interface from both a kinematic and dynamic perspective and to compare three robots for use as a 5-DOF haptic pen. The algorithm demonstrates consistent effort reductions of up to six orders of magnitude over global searching with low sensitivity to initial conditions.

## INTRODUCTION

Modern robot applications such as haptic interfaces make performance demands far beyond those of the assembly and repetitive task devices of the past. Meeting these demands is difficult because robot capabilities tend to degrade at certain configurations or when acting in certain directions. Geometric parameters largely determine how consistently a robot behaves and many proposals have been made regarding how to choose these parameters. Cost functions have been proposed to describe kinematic isotropy, manipulability and accuracy (Kim and Khosla, 1991), inertial isotropy and stiffness (Angeles et. al., 1992), kinematic nonlinearity and redundancy (van den Doel and Pai, 1994) and maximum joint velocity (Merlet, 1996). Various ways of removing the configuration dependence from these measures have also been proposed. They include integrating over the workspace (Gosselin and Angeles, 1991) which results in an average and tends to tolerate small regions with poor behaviour, worst-case values (Hayward et. al., 1994) which due the local nature of the measure does not consider relative performance between configurations and the number of poses where performance surpasses a threshold value (Kircanski, 1994), which ignores behaviour in the remainder of the workspace. In this paper, the shortcomings of these methods are circumvented by defining a new cost function that does not consider configurations individually but, instead, compares worst-case values of the workspace as a whole. The cost function is calculated from the singular values of the Jacobian or mass matrix which is scaled to homogenize the physical units, tailor it a specific application and allow inclusion of actuator parameters into the optimization search space. The cost function and a new optimization algorithm are used to optimize the kinematic designs of a 5-DOF haptic interface and the kinematic and dynamic design of a 2-DOF pantograph haptic interface.

A proposal for normalizing and scaling the Jacobian or mass matrix is followed by a description of a new measure of global isotropy. A global search method is presented to search a discretized parameter and workspace for the optimum. Unlike descent based optimization algorithms, this method is unhampered by non-differentiable, non-convex or discontinuous cost functions or those that contain local minima. Two versions are given to perform optimization of the new global measure or to solve problems of the minimax form. The cost function and a new optimization algorithm are used to optimize the kinematic designs of a 5-DOF haptic interface and the kinematic and dynamic design of a 2-DOF pantograph haptic interface.

## PERFORMANCE MEASURES

Isotropy is often computed by the ratio of singular values at a position $x$ for a design parameter $p$. For example, the ratio $\sigma_{min}(J(x, p))/\sigma_{max}(J(x, p))$ compares the magnitudes of the major and minor axes of the position dependent velocity ellipsoid. This is a local isotropy measure and manipulators designed to be isotropic at individual points may not exhibit similar levels of isotropy throughout their workspaces. In the past (Hayward et. al., 1994), configuration independence has been checked by the secondary local measure $\sigma_{min}\sigma_{max}$. Here, this secondary measure is averted by introducing a global isotropy index (*GII*) which compares the smallest singular value in the workspace to the largest (Eq. (1)). The *GII* extends the idea that robot performance at a configuration can be summarized by the lengths of its major and minor velocity ellipsoid axes to encompass the entire workspace.

$$GII(p) = \frac{\Psi(p)}{\Lambda(p)} = \frac{\underset{x \in W}{min}\ \underline{s}(p,x)}{\underset{x \in W}{max}\ \tilde{s}(p,x)} \quad (1)$$

$$\underline{s}(p,x) = \sigma_{min}[J(p,x) \text{ or } D(p,x)]$$

$$\tilde{s}(p,x) = \sigma_{max}[J(p,x) \text{ or } D(p,x)]$$

For example, consider the constrained (workspace limited to a horizontal trajectory) elbow manipulator in Fig. 1. Local velocity ellipsoids map all arbitrarily oriented, unit magnitude, end-effector velocities at a particular configuration into joint rates. The *GII* is the ratio of the radius of the largest sphere contained in all these ellipsoids to the radius of the smallest sphere containing all these ellipsoids. Figure 2 shows velocity ellipsoids and spheres for the robot and workspace shown in Fig. 1.

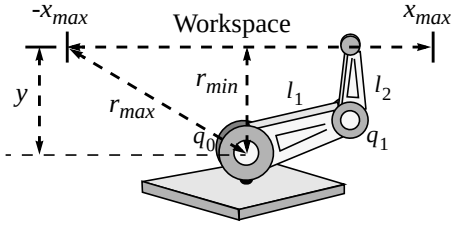


**Figure 1: Constrained Elbow Manipulator Example**

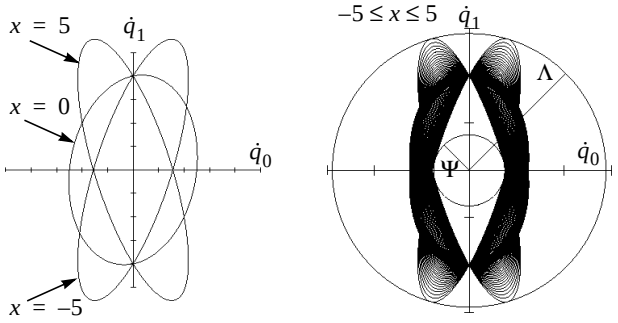


**Figure 2: Velocity Ellipsoids**

A globally isotropic robot design parameter is one that maximizes the *GII* as in Eq. (2).

$$p_{optimum} = \underset{p \in P_0}{\arg max}\ GII(p) \quad (2)$$

Note that the *GII* only considers the ratio between worst-case singular values but ignores other issues that may also be important such as magnitude or smoothness. If necessary, these should be checked as secondary measures after an optimal *GII* has been obtained or be included with scale factors into the original cost function.

The task of a haptic interface is to present virtual impedances to a human hand. It can be simply modeled by the equivalent circuit in Fig. 3 where $\tau$ is the actuator torque, $Z_R$ is the configuration dependent robot impedance, $f_H$ is the force applied by the hand and $Z_E$ is the equivalent impedance perceived by the hand.

Using the Jacobian definition of Eq. (3) for a parallel manipulator, the actuator torque $\tau$ required to produce an equivalent impedance $Z_E$, assuming the relationship between applied force and perceived

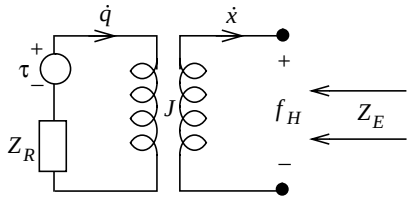


**Figure 3: Equivalent Circuit of Haptic System**

impedance in Eq. (4), is given in Eq. (5). Ideally, one would like the control law that emulates the impedance $Z_E$ to be both isotropic (position independent) and direction independent. Since Eq. (5) suggests that the equivalent actuator impedance is dictated to a large extent by the Jacobian, these desired characteristics can be achieved by optimizing *J* to satisfy the same criteria.

$$\dot{q} = J\dot{x} \quad (3)$$

$$f_H = -Z_E\dot{x} \quad (4)$$

$$\tau = Z_R J\dot{x} + J^{-T} Z_E \dot{x} \quad (5)$$

The interpretation of the Jacobian in Eq. (3) can also be used to indicate kinematic accuracy and distance from singular positions while a dual force/torque interpretation can be used to indicate the distribution of power among actuators for forces of constant magnitude and arbitrary direction at the end-effector. Both of these have a direct relationship to the controllability of the device and support the claim that robot performance improves when the Jacobian is more isotropic and well conditioned.

The conditioning of *J* can be checked by comparing its minimum and maximum singular values. The singular values are, however, only meaningful when the physical units are homogeneous. This is not the case when a manipulator is capable of both translation and rotation at its end effector. This has led to various proposals to normalize the units using a quantity known as “characteristic link length”. They include choosing the characteristic link length which produces the best condition number (Angeles et. al., 1992) and using the average platform radius (Ma and Angeles, 1991) for a parallel manipulator. In both cases, dimensional weighting is chosen in such a way as to place equal demands upon the actuators in either domain. Relative robot capabilities should not be determined in this way but should, instead, reflect the demands of the application. Also, the optimal solution will not always involve identical actuators which is a further constraint. This is particularly obvious if one is designing a serial mechanism.

A different approach is to pre and post-multiply *J* by two diagonal weighting matrices, $\Omega$ and $\Gamma$. The diagonal entries of these matrices represent maximum values for the two vectors related by *J*. For example, in the kinematic relationship of Eq. (3), the two matrices have the physical interpretation shown in Eq. (6) and Eq. (7). The resulting normalized Jacobian transforms two dimensionless vectors, $\Delta\dot{q}$ and $\Delta\dot{x}$, which represent percentages of maximum physical values. Not only are the physical units homogeneous but dissimilar physical dimensions are ranked explicitly with respect to the demands of the application. Relative actuator requirements can also be solved by

including them in the vector of design parameter $p$ searched by the optimization algorithm.

$$\Omega^{-1}\Delta\dot{q} = J\Gamma\ \Delta\dot{x} \tag{6}$$

$$\Delta\dot{q} = \Omega J\Gamma\ \Delta\dot{x} \tag{7}$$

Since scalar multiples do not affect isotropy, they can be factored out to produce normalized, diagonal, transformation matrices of relative weightings. Example 2-DOF matrices for Eq. (7) are shown in Eq. (8) and Eq. (9) where $\dot{q}_{max}$ is a vector of maximum velocities of two actuators denoted by subscripts *0* and *1* and $\dot{x}_{max,\,lin}$ and $\dot{x}_{max,\,ang}$ are the maximum linear and angular velocities.

$$\Omega^{-1} = \begin{bmatrix} \dot{q}_{max,\,0} & 0 \\ 0 & \dot{q}_{max,\,1} \end{bmatrix} = \dot{q}_{max,\,0}\begin{bmatrix} 1 & 0 \\ 0 & \dot{q}_{max,\,1}/\dot{q}_{max,\,0} \end{bmatrix} \tag{8}$$

$$\Gamma = \begin{bmatrix} \dot{x}_{max,\,lin} & 0 \\ 0 & \dot{x}_{max,\,ang} \end{bmatrix} = \dot{x}_{max,\,lin}\begin{bmatrix} 1 & 0 \\ 0 & \dot{x}_{max,\,ang}/\dot{x}_{max,\,lin} \end{bmatrix} \tag{9}$$

The $\Omega$ matrix is diagonal and usually describes either relative actuator velocity or torque. When it is included, its diagonal entries are added to the design parameter search vector $p$, so that $p$ contains both geometric quantities and actuator scale factors. The values chosen by optimization can be implemented, for example, by adding reduction mechanisms or by scaling the actuators themselves, both of which increase rotor inertia and may hamper performance. Limits should, therefore, be placed on the values that are searched to match an actuation strategy that will not overly impact performance. If, for example, direct drive is required, ratios should be constrained to *2* or *3:1* whereas if planetary or harmonic drives can be used, ratios of up to *20:1* or *200:1* are reasonable.

## CULLING ALGORITHM

Descent and stochastic algorithms are not well suited to robot mechanism design problems. Descent algorithms can not reliably avoid the abundance of local minima and stochastic approaches offer only a measures of confidence rather than a guarantee of global optimality. A new algorithm is proposed which is essentially an accelerated global search. It identifies non-optimal parameters and culls them from the search space until only the optimum remains. The algorithm optimizes the *GII* (Eq. (1)) which is defined between *0* and *1* corresponding to poor and ideal performance respectively over a workspace $W$ which is a constrained set of configurations $x$ for a parameter $p$. The optimization goal (Eq. (2)) is to find the parameter $p$ with the best "worst-case" behavior throughout the constrained workspace $W$. The algorithm is shown in Eq. (10) through Eq. (19).

After some initialization (Eq. (10) and Eq. (11)), a starting guess $p_0$ is chosen (Eq. (12)). Performance indices are calculated for $p_i$ at each $x$ in $W$ (Eq. (13)). If $p_i$ shows better worst-case performance than the front-runner $\hat{p}_i$, $p_i$ becomes the new front-runner $\hat{p}_{i+1}$ (Eq. (14)). Performance indices are calculated for each $p$ in $P_i$ at $\underset{\sim}{x}_i$ and $\tilde{x}_i$ and the corresponding worst-case-so-far indices $\underset{\sim}{S}_i(p)$ and $\tilde{S}_i(p)$ are updated (Eq. (15)). Equation (15) is omitted for all $p$ whose worst-case-so-far performance is worse than $\Psi(\hat{p}_{i+1})/\Lambda(\hat{p}_{i+1})$ since they are culled from $P_i$ in Eq. (16). The $p$ with the best worst-case-so-far performance is chosen as the next candidate $p_{i+1}$ (Eq. (17)). Equation (13) through Eq. (18) are repeated until $\hat{p}_i$ is the only parameter left in $P_i$ at which point $\hat{p}_i$ is the global optimum (Eq. (19)).

**GII Culling Algorithm**

$$i = 0 \tag{10}$$

$$\underset{\sim}{S}_0(p \in P_0) = \infty \qquad \tilde{S}_0(p \in P_0) = 0 \tag{11}$$

$$(p_0 = \hat{p}_0) \in P_0 \tag{12}$$

REPEAT

$$\underset{\sim}{x}_i = \underset{x \in W}{\arg min}\ \underset{\sim}{s}(p_i, x) \qquad \tilde{x}_i = \underset{x \in W}{\arg max}\ \tilde{s}(p_i, x) \tag{13}$$

$$\hat{p}_{i+1} = \begin{cases} p_i \text{ if } \dfrac{\Psi(p_i)}{\Lambda(p_i)} > \dfrac{\Psi(\hat{p}_i)}{\Lambda(\hat{p}_i)} \\ \hat{p}_i \text{ otherwise} \end{cases} \tag{14}$$

$$\underset{\sim}{S}_{i+1}(p) = \underset{p \in P_i}{min}\ \{\underset{\sim}{S}_i(p), \underset{\sim}{s}(p, \underset{\sim}{x}_i), \underset{\sim}{s}(p, \tilde{x}_i)\}$$

$$\tilde{S}_{i+1}(p) = \underset{p \in P_i}{max}\ \{\tilde{S}_i(p), \tilde{s}(p, \underset{\sim}{x}_i), \tilde{s}(p, \tilde{x}_i)\} \tag{15}$$

$$P_{i+1} = \left\{ p \in P_i \mid \frac{\underset{\sim}{S}_{i+1}(p)}{\tilde{S}_{i+1}(p)} \geq \frac{\Psi(\hat{p}_{i+1})}{\Lambda(\hat{p}_{i+1})} \right\} \tag{16}$$

$$p_{i+1} = \underset{p \in P_{i+1}}{\arg max}\ \frac{\underset{\sim}{S}_{i+1}(p)}{\tilde{S}_{i+1}(p)} \tag{17}$$

$$i = i + 1 \tag{18}$$

UNTIL $\hat{p}_i = p_i$ (19)

Since parameters are removed from the search space only after exhibiting worse behaviour than another parameter for which the absolute worst-case has been rigorously computed, the global optimum is guaranteed. Computational savings result from strategically exploring configurations which are likely to eliminate many sub-optimal parameters simultaneously. The level of expected success, however, relies on the presumption that within a continuous, bounded range of parameters, many (particularly those in close proximity to each other) will exhibit similar behaviour at similar configurations.

While the GII culling algorithm is specifically tailored for *GII* optimization, some worst-case design are of the form shown in Eq. (20) and can be solved using a similar approach. An optimization criteria of this form is used, for example, by (Hayward et. al., 1994) with $s(p, x) = \sigma_{min}(D(x, p))/\sigma_{max}(D(x, p))$ to optimize the mass matrix of a planar pantograph haptic interface. The minimax culling algorithm is shown in Eq. (21) through Eq. (30).

$$p_{optimum} = \underset{p \in P_0}{\arg max}\ \underset{x \in W}{min}\ s(p, x) \tag{20}$$

## APPLICATION TO A PLANAR HAPTIC INTERFACE

In (Hayward et. al., 1994) a five-bar linkage is optimized for use as a planar haptic interface. The culling algorithm and new definition of global isotropy are used to re-examine this mechanism for both kinematic and dynamic conditioning. A general representation of a five-bar linkage with a square workspace (Fig. 4) is used to establish symmetry and positioning guidelines.

**Minimax Culling Algorithm**

$$i = 0 \tag{21}$$

$$S_0(p) = 1, \forall\ p \in P_0 \tag{22}$$

$$(p_0 = \hat{p}_0) \in P_0 \tag{23}$$

REPEAT

$$x_i = \underset{x \in W}{\arg min}\ s(p_i, x) \tag{24}$$

$$\hat{p}_{i+1} = \begin{cases} p_i & \text{if } \Psi(p_i) > \Psi(\hat{p}_i) \\ \hat{p}_i & \text{otherwise} \end{cases} \tag{25}$$

$$S_{i+1}(p) = \min_{p \in P_i} \{S_i(p), s(p, x_i)\} \tag{26}$$

$$P_{i+1} = \{p \in P_i \mid (S_{i+1}(p) \geq \Psi(\hat{p}_{i+1}))\} \tag{27}$$

$$p_{i+1} = \underset{p \in P_{i+1}}{\arg max}\ S_{i+1}(p) \tag{28}$$

$$i = i + 1 \tag{29}$$

UNTIL $\hat{p}_i = p_i$ (30)

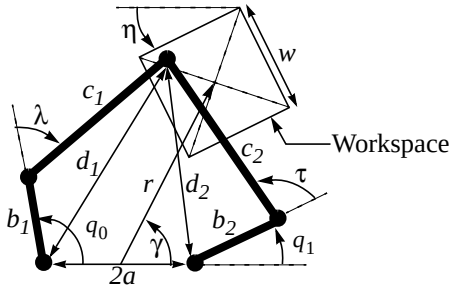


**Figure 4: Generalized Five-Bar Linkage**

The kinematic *GII* is optimized with seven free parameters ($a$, $b_1$, $b_2$, $c_1$, $c_2$, $\gamma$ and $\eta$) with $r$ and $w$ fixed to avoid a trivial result (i.e. isotropy improves as $r \to \infty$ or as $w \to 0$) and $\Omega$ and $\Gamma$ set to the identity (identical actuators and equal capabilities in both directions). For $r=w=10$ and $\Delta w=0.1$ ($\Delta w$ is the discrete sample spacing in the workspace*)* the search space and global optimum obtained by the GII culling algorithm are shown in Table 1.

**Table 1: Parameter Space & Optimum**

| Parameter | Min. Val. | Max. Val. | Resolution | Optimum |
|---|---|---|---|---|
| a | 0 | 3 | 0.5 | 1.5 |
| $b_1$, $b_2$ | 4 | 10 | 0.5 | 7.5 |
| $c_1$, $c_2$ | 7 | 14 | 0.5 | 9.5 |
| $\gamma$, $\eta$ | 0 | $\pi/2$ | $\pi/20$ | $\pi/2$ |

The global optimum has left/right symmetry of both the robot and workspace. Future optimizations, therefore, need only consider three parameters ($a$, $b=b_1=b_2$ and $c=c_1=c_2$) and half of the workspace. This simplifies the problem sufficiently to allow further generalization. Varying $r$ while constraining the elbow angles to $0 \leq (\lambda, \tau) \leq \pi$ shows the optimum posture for different values of $r$. Figure 5 shows the optimum geometry, *GII* and posture for $-25 \leq r \leq 25$, $\gamma=\eta=\pi/2$ and the parameter space shown in Table 2. Note that the search space constrains the robot and workspace to a *30*x*30* square area.

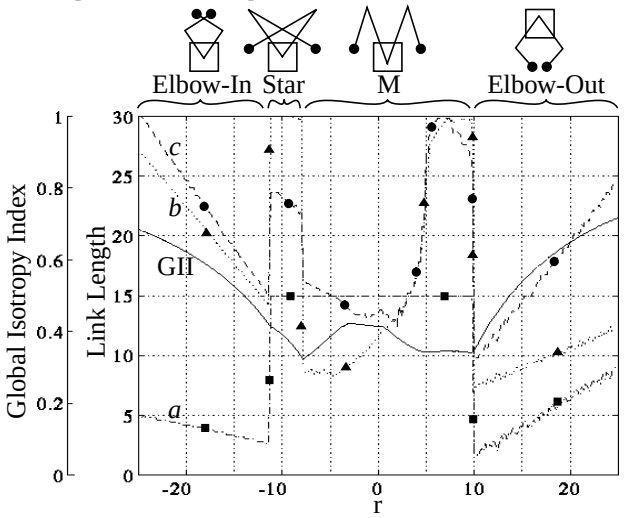


**Figure 5: Optimal Postures of Five-Bar Linkage**

**Table 2: Reduced Parameter Space**

| Parameter | Min. Val. | Max. Val. | Resolution |
|---|---|---|---|
| *a* | 0 | 15 | 0.2 |
| *b, c* | 5 | 30 | 0.2 |

The *GII* curve is non-smooth and the optimal parameter curves (*a, b* & *c*) are discontinuous in *r.* Parametric discontinuities occur at the intersections of optimum *GII* curves for different postures. Consider the region around *r=10*. The optimum *GII* of the "M" posture is relatively level while the optimum *GII* of the elbow-out posture logarithmically increases with *r*. When the curves intersect, the optimum posture switches from "M" to elbow-out and the parametric curves experience a jump.

There are clearly two viable ranges for *r.* Magnitudes less than 5 are acceptable in which case the "M" posture is best with the workspace positioned below the actuators. Magnitudes greater than 10 are also acceptable in which case the elbow-out posture is preferred. While elbow-in achieves *GII*s similar to elbow-out for similar magnitudes of *r* it requires longer physical link lengths (*b* & *c*). The inertial implications of this distinguish elbow-out as the better posture. For magnitudes between 5 and 10, the optimal postures combine long link lengths with poor *GII*s and should be avoided.

An inertial optimization is next carried out which assumes a light, fingertip grip and, therefore neglects hand inertia. The mass matrix is obtained by solving the elbow joint velocities and computing the mass matrices of the two elbow manipulators (Spong and Vidyasagar, 1989) making up the five-bar linkage. The robot's natural frequency is conservatively bounded by choosing the beam dimensions that place the same lower bound on the natural frequency $\omega$ of a cantilever beam the length of all four robot links arranged end to end (Hunt, 1979). The diameter $d$ and mass/unit length $m$ are calculated assuming circular cross-section 2024-T4 aluminum tubing of thickness $t$.

$$d = 2.55 \times 10^{-6} (b_1 + b_2 + c_1 + c_2)^2 \omega \text{ (cm)}$$
$$m = 8.7dt \text{ (g/cm)}$$

It is debatable whether it is preferable to optimize the mass matrix for isotropy or scale. Since isotropic mass is not particularly important

if the magnitude is small, it is decided to minimize maximum mass by considering the normalized performance index involving only the maximum singular value of the mass matrix shown in Eq. (31). Since this measure does not involve a workspace inclusive ratio of singular values, the minimax culling algorithm can be used. The measure is optimized with $w=10$, $\Delta w=0.1$ and $\omega=200\pi$ (*100* Hz).

$$s(p, x) = \frac{1}{1 + \sigma_{max}[D(p, x)]} \tag{31}$$

Two different parameter spaces are searched. The first has one free parameter *r* which is matched to its corresponding kinematic optimum robot geometry (*a*, *b* and *c*) from Fig. 5. The second parameter space is comprised of a much larger cross-section (all 4 dimensions free) of geometric combinations. Note that although a trivial result is obtained when *r* is free during kinematic optimization, this does not occur during dynamic optimization. The two parameter spaces are shown in Table 3.

**Table 3: Inertial Parameter Spaces & Optima**

| Parameter | Min. Val. | Max. Val. | Resolution | Optimum |
|---|---|---|---|---|
| Parameter Space #1 | | | | |
| *a* | n/a | n/a | n/a | 1.6 |
| *b* | n/a | n/a | n/a | 7.6 |
| *c* | n/a | n/a | n/a | 9.8 |
| *r* | -25 | 25 | 0.2 | 10.4 |
| Parameter Space #2 | | | | |
| *a* | 0 | 15 | 0.2 | 0 |
| *b* | 5 | 30 | 0.2 | 7.2 |
| *c* | 5 | 30 | 0.2 | 8.8 |
| *r* | -25 | 25 | 0.2 | 9.2 |

The first parameter space has a very narrow scope but guarantees a kinematically favourable solution. The second ignores kinematic conditioning but results in the dynamic global optimum. In order to choose between the two, they are compared using the sensitivity analysis in Table 4. Since solution "A" shows a smaller decrease in dynamic performance than solution "B" shows in kinematic performance, solution "A" (*a=1.6, b=7.6, c=9.8, r=10.4*) is concluded to offer the best overall performance.

**Table 4: Sensitivity Analysis**

| | Kinematic GII | Inertia Index |
|---|---|---|
| Solution A - Parameter Space #1 | 0.3657 | 0.9045 |
| Solution B- Parameter Space #2 | 0.2790 | 0.9271 |
| Sensitivity (% change) | -23.7% | +2.5% |

As previously mentioned, haptic interface performance may also be hampered by sudden changes in singular values. This is checked as a secondary measure by plotting the minimum and maximum singular values of the Jacobian and mass matrices over the workspace. As seen in Fig. 6, they are both smooth and even have regions of perfect local isotropy where the minimum and maximum singular value curves intersect ($\sigma_{max} = \sigma_{min}$).

## OPTIMIZATION OF A 5-DOF HAPTIC INTERFACE

With fast global optimization, one can not only select optimal robot parameters but also the optimal robot. By optimizing a number of

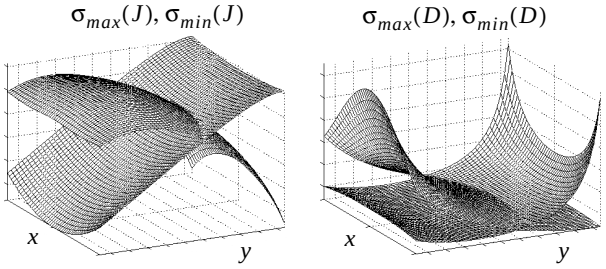


**Figure 6: Singular Values of Jacobian & Mass Matrix**

candidates, one can choose the device whose capabilities best suit a particular application. In (Stocco and Salcudean, 1996), three devices are compared in terms of their reachable workspaces to act as the coarse stage in a coarse-fine haptic pen. They including the "Stewart" platform (Fichter, 1986), a five-bar linkage actuated "Spider" platform (Tsusaka et. al., 1987), and a novel mechanism called the "Twin-Elbow" platform (Stocco and Salcudean, 1996). These three devices are shown in Fig. 7 through Fig. 9.

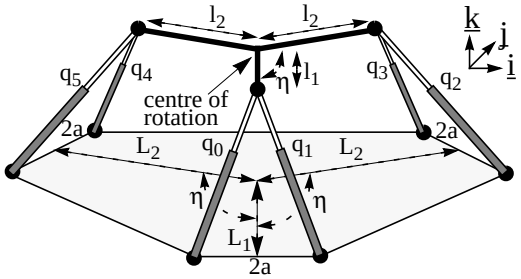


**Figure 7: Stewart Platform**

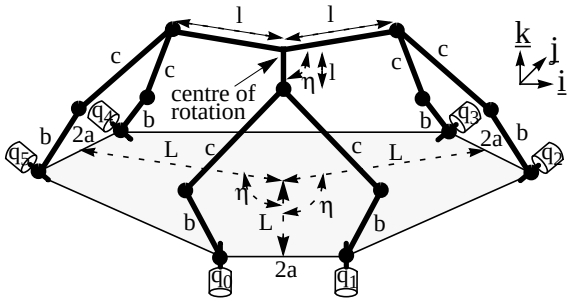


**Figure 8: Spider Platform**

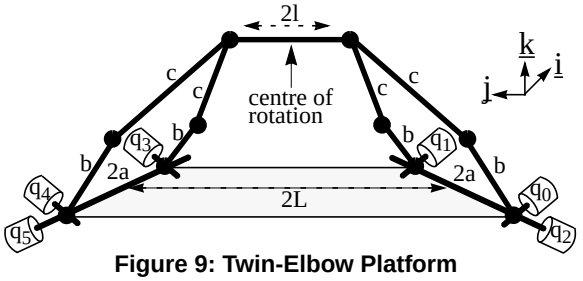


**Figure 9: Twin-Elbow Platform**

The pen axis aligns with the $j$ axis of the coarse stage robot at its home position. It is desirable to have unrestricted ability to rotate about the pen axis in applications such as virtual or tele-operated surgery where one must orient the cutting direction of a scalpel. This is accommodated by using a series actuator to provide that degree of freedom. The candidates are, therefore, only compared with respect to

their remaining five degrees of freedom. Since the chosen device will act essentially as a velocity source, the three are compared in terms of their Jacobian velocity transformations shown in Eq. (7).

A literature survey of suggested design goals for a haptic interface and experimental results showing the linear motion capabilities of the human hand can be found in (Stocco and Salcudean, 1996). To clarify rotational capabilities with respect to workspace size, an angular version of the experiment was conducted. Ten subjects were asked to oscillate their wrists at various amplitudes as fast as possible while the trajectories were recorded by a low mechanical impedance potentiometer. The maximum velocity achieved at each amplitude is calculated from the corresponding average frequency by assuming a sinusoidal trajectory as in Eq. (32). The results of this transformation are shown in Fig. 10.

$$x = A\sin(\omega t) \qquad \|v\| = A\omega \qquad (32)$$
$$v = \dot{x} = A\omega\cos(\omega t)$$

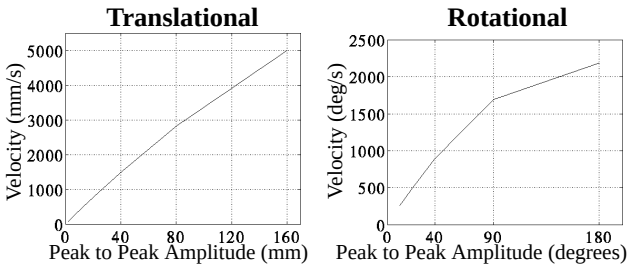


**Figure 10: Human Capability vs. Motion Range**

It was proposed in (Stocco and Salcudean, 1996) that a reasonable workspace size for such a device is *16 cm* ( $\underline{i}$ axis) × *10 cm* ( $\underline{j}$ / $\underline{k}$ axes) × ±*45*° (pitch / yaw). From Fig. 10, the following maximum velocities are expected for this motion range.

$$\dot{x}_{max} = 500 \text{ cm/sec (@ 16 cm)}$$
$$\omega_{max} = 29.67 \text{ rad/sec (@ 90° p-p)}$$
$$R = \frac{\omega_{max}}{\dot{x}_{max}} = 5.93\times10^{-2}\text{rad/cm}$$

Each manipulator is allotted one free actuator scale factor *Q*. *Q* is applied to the waist joints of the Twin-Elbow platform and the two front joints of the Stewart and Spider platforms since they have left-right symmetry but lack front/back symmetry. The kinematic *GII* of each robot is optimized using the normalized Jacobians shown in Eq. (33) and Eq. (34). Note that due to redundancy in all three robots, the Jacobians are 6×5 matrices.

$$\hat{J}_{Twin-Elbow} = \Omega_{TE} J \Gamma \qquad (33)$$
$$\hat{J}_{Stewart,\,Spider} = \Omega_S J \Gamma \qquad (34)$$
$$\Omega_{TE} = Diag(\begin{bmatrix}1 & 1 & Q & 1 & 1 & Q\end{bmatrix})$$
$$\Omega_S = Diag(\begin{bmatrix}Q & Q & 1 & 1 & 1 & 1\end{bmatrix})$$
$$\Gamma = Diag(\begin{bmatrix}1 & 1 & 1 & R & R\end{bmatrix})$$

The GII culling algorithm is used to optimize the *GII* of each robot with the workspace centred *25 cm* above the base. As with the planar device, the workspace position must be fixed to avoid a trivial result. The search spaces and optimum geometries are shown in Table 5 while Table 6 compares the three kinematically optimized devices in terms of their resultant *GII*s and combined total link lengths (this correlates to total moving mass) which is indicative of the relative amounts of inertia one can expect to experience from similarly constructed devices.

**Table 5: Kinematic Optimizations**

| Parameter | Min. | Max. | Res. | Opt. |
|---|---|---|---|---|
| Candidate #1 - Stewart Platform: | | | | |
| a | 2 | 30 | 1 | 14 |
| $L_1$ | 2 | 15 | 0.5 | 8 |
| $L_2$ | 2 | 15 | 0.5 | 10.5 |
| $L_1/l_1$, $L_2/l_2$ | 0.1 | 2 | 0.1 | 0.5 |
| η | 100° | 140° | 5° | 120° |
| Q | 0.7 | 1.3 | 0.1 | 1.1 |
| Candidate #2 - Spider Platform: | | | | |
| a | 0.5 | 4 | 0.5 | 0.5 |
| b | 10 | 30 | 1 | 18 |
| c | 15 | 35 | 1 | 24 |
| L | 2 | 12 | 1 | 7 |
| L/l | 0.2 | 1.3 | 0.1 | 0.6 |
| η | 100° | 150° | 5° | 135 |
| Q | 0.7 | 1.2 | 0.1 | 0.9 |
| Candidate #3 - Twin-Elbow Platform: | | | | |
| a | 0.25 | 5 | 0.25 | 2.75 |
| b | 10 | 30 | 0.5 | 18.5 |
| c | 10 | 35 | 0.5 | 23 |
| l, L | 5 | 20 | 0.5 | 10.5 |
| Q | 0.5 | 2 | 0.1 | 1.6 |

**Table 6: 5-DOF Optimization Results**

| | Stewart | Spider | Twin-Elbow |
|---|---|---|---|
| Sum total of all link lengths | $6q_{max}+l_1+2l_2$ = 347.8 cm | $6(b+c)+3l$ = 287 cm | $4(b+c)+2l$ = 187 cm |
| GII | 0.236 | 0.191 | 0.283 |

The Twin-Elbow platform is superior to the other two devices in both respects and also has two actuators which are base mounted, making a smaller inertial contribution to the system. The Stewart platform has leg lengths ranging between *10.8* and *48.3 cm* requiring the actuators to extend below the base where they could intersect and the Spider platform can experience interferences between adjacent pantograph elbows. This does not occur with the Twin-Elbow since its pantographs face one another so it is also less prone to linkage collisions.

For the Twin-Elbow platform, an optimal value of *Q = 1.6* was obtained. This indicates that the waist actuators rotate an average of 1.6 times slower than the shoulders. If used, reduction mechanism should, therefore, have ratios *1.6* times larger at the waist joints to obtain isotropic velocities at the actuator shafts. Also, if measurements are taken directly at the joints, a similar increase in sensor resolution is required to ensure isotropic measurement accuracy.

A prototype Twin-Elbow platform based 5-DOF haptic interface with passive roll has been constructed for experimental purposes. Its end-effector is oriented vertically to offer a more natural pen/probe

grip, to accommodate gravitational counterbalancing and to shift the gravitational burden onto the stronger and redundantly over-actuated waist joints. Robot mass is minimized through the use of carbon fibre links, magnesium clevises and titanium wrist pins. A photograph of the prototype haptic interface is shown in Fig. 11.

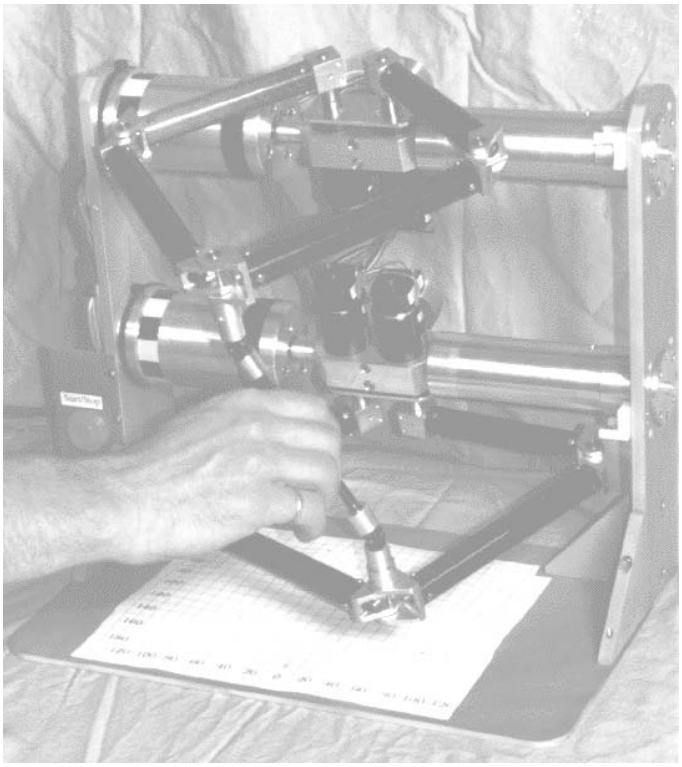

**Figure 11: Prototype Haptic Pen**

## EFFICIENCY OF CULLING ALGORITHM

The culling algorithm is essentially a global search that avoids redundant evaluations. Therefore, it always converges to the global optimum within the discretized parameter space. Each loop iteration removes at least one parameter from contention so the number of potential loop iterations is bounded by the dimension of the parameter space and the stopping criterion is always satisfied in finite time. A worst-case scenario of no culling whatsoever results in an exhaustive global search. As with most optimization algorithms, efficiency depends on the objective function and initial conditions. While the algorithm makes no efficiency guarantees, experience with robot design problems has shown consistently dramatic improvement over a global search with low sensitivity to initial conditions. Table 7 compares the number of condition index calculations performed by the culling algorithm to those required by a global search for the optimizations discussed in this paper.

**Table 7: Culling/Global Search Efficiency**

| Optimization | Workspace Size | Param Space Size | Search : Cull Ratio |
|---|---|---|---|
| Table 1 | $1.02\times10^{4}$ | $2.66\times10^{7}$ | 3670 : 1 |
| Table 2 | 5151 | $1.21\times10^{6}$ | $1910^{A}$ : 1 |
| Table 3 - #1 | 5151 | 251 | 82 : 1 |
| Table 3 - #2 | 5151 | $3.03\times10^{8}$ | $3500^{B}$ : 1 |
| Table 5 - #1 | $4.00\times10^{6}$ | $2.28\times10^{7}$ | $1.85\times10^{6}$ : 1 |
| Table 5 - #2 | $4.00\times10^{6}$ | $2.82\times10^{7}$ | $1.54\times10^{6}$ : 1 |
| Table 5 - #3 | $2.10\times10^{6}$ | $2.07\times10^{7}$ | $1.25\times10^{6}$ : 1 |

*A. Typical value for an optimization conducted for any one value of r*

*B. The parameter space was divided into 10 parts to overcome hardware (memory) limitations so the reported ratio is an average. Partitioning reduces the efficiency of the culling algorithm so the reported improvement ratio is conservative.*

One should not try to improve efficiency by replacing the global workspace search of each candidate parameter by a faster, possibly stochastic approach. This will eliminate the guarantee of global optimality and reduce the severity of culling each time a suboptimal worst-case position is found, compensating, or possibly even overcompensating for performance gains resulting from the faster search.

## CONCLUSIONS

A new global isotropy index (*GII*) is proposed which defines isotropy as the ratio between the minimum and maximum singular values in the workspace. It summarizes the global performance of a mechanism by a scalar and can be applied to either the Jacobian or mass matrix. The physical units of the matrix can be normalized and tailored to a specific set of requirements by post-multiplying it by a diagonal scaling matrix. Optimal actuator scaling factors (transmission ratios) can also be solved simultaneously with geometric parameters by pre-multiplying the matrix by a diagonal scaling matrix of free variables.

A novel optimization procedure is also proposed which is a variation of the global search method. It repeatedly uses the worst configuration of one parameter to eliminate others from contention until only the optimum remains. The approach guarantees convergence, finite time termination and a global result. Two versions of the algorithm are presented for optimization of either the *GII* or some other local measure. The algorithm consistently demonstrates drastic improvements over global searches with observed ratios of up to *1,850,000 : 1.* An optimization (Table 5 - #1) that took approximately *3* days to solve on a Sparc 5 workstation using the culling algorithm is estimated to require *15,000* years to solve by global search on a similar machine. The culling algorithm, therefore, allows one to use unsophisticated computer hardware to solve high dimensional problems that would otherwise be too computationally demanding to attempt.

The kinematic *GII* and maximum inertia of a five-bar linkage based planar haptic interface are optimized. It is shown that the best overall architecture has left/right symmetry about the robot and workspace and that the robot is best kept in either an “M” or elbow-out posture. A sensitivity analysis is performed to trade-off kinematic and dynamic performance for an overall optimum design. Kinematic optimizations of a Stewart platform, Spider platform and a hybrid serial/parallel device called the Twin-Elbow show that the Twin-Elbow

platform is the most viable candidate for use as the coarse stage of a coarse-fine haptic pen.

## ACKNOWLEDGEMENTS

The authors would like to thank Dr. Philip D. Loewen for his comments during the revision of the manuscript. This work is supported by the HMI-6 and IS-8 Canadian IRIS Network of Centres of Excellence projects.

## REFERENCES

Angeles, J., Ranjbaran, F., Patel, R.V., "On the Design of the Kinematic Structure of Seven-Axes Redundant Manipulators for Maximum Conditioning", Proceedings of IEEE International Conference on Robotics and Automation (Nice, France), pp. 494-499, May 10-15, 1992.

van den Doel, K., Pai, D.K., "Constructing Performance Measures for Robotic Manipulators", Proceedings of IROS '94, IEEE/RSJ/GI International Conference on Intelligent Robots qnd Systems, Advances in Robotic Sytems and the Real World (Munich, Germany), pp.1601-1607, Sept. 12-16, 1994.

van den Doel, K., Pai, D.K., "Redundancy and Non-linearity Measures for Robot Manipulators", Proceedings of IEEE International Conference on Robotics and Automation (San Diego, California), pp. 1873-1880, May 8-13, 1994.

Fichter, E.F., "A Stewart Platform-Based Manipulator: General Theory and Practical Construction", Int. Journal of Robotics Reserve, Vol. 5, No. 2, pp. 157-182, 1986.

Gosselin, C., Angeles, J., "A Global Performance Index for the Kinematic Optimization of Robot Manipulators", Transactions of ASME, Journal of Mechanical Design, Vol. 113, pp. 220-226, Sept. 1991.

Hayward, V., Choksi, J., Lanvin, G., Ramstein, C., "Design and Multi-Objective Optimization of a Linkage for a Haptic Interface", Proceedings of ARK '94, 4th International Workshop on Advances in Robot Kinematics (Ljubliana, Slovenia), Jun. 1994.

Hunt, J.B., "Dynamic Vibration Absorbers", Mechanical Engineering Publications, 1979.

Kim, J-O., Khosla, P.K., "Dexterity Measures for Design and Control of Manipulators", Proceedings of IROS '91, IEEE/RSJ International Workshop on Intelligent Robots and Systems (Osaka, Japan), pp. 758-763, Nov. 3-5, 1991.

Kircanski, M.V., "Robotic Isotropy and Optimal Robot Design of Planar Manipulators", Proceedings of IEEE International Conference on Robotics and Automation (San Diego, California), pp. 1100-1105, May 8-13, 1994.

Ma, O., Angeles, J., "Optimum Architecture Design of Platform Manipulators", Proceedings of ICAR '91, 5th International Conference on Advances in Robotics. Robots in Unstructured Environments (Pisa, Italy), pp. 1130-1135, June 19-22, 1991.

Merlet, J-P., "A DEsign MethOdology for the Conception of Robot with parallel ArchiTecture", Internal Report, INRIA Sophia-Antipolis, 1996.

Spong, M.W., Vidyasagar, M., "Robot Dynamics and Control", John Wiley & Sons, 1989.

Stocco, L., Salcudean, S.E., "A Coarse-Fine Approach to Force-Reflecting Hand Controller Design", Proceedings of IEEE International Conference on Robotics and Automation (Minneapolis, Minnesota), Vol. 1, pp. 404-410, Apr. 22-28, 1996.

Tsusaka, Y., Fukuizumi, T., Inoue, H., "Parallel Manipulator: Its Design and Mechanical Characteristics, ", Journal of Robotics Society of Japan, Vol. 5, No. 3, 1987.